Acta Geod. Geoph. Mont. Hung., Vol. 24 (3-4), pp. 213-236 (1989)

ON THE RELATION BETWEEN THE GRAVITY FIELD AND LITHOSPHERIC FEATURES IN THE GREEK AREA

M Doufexopoulou, P Milas, B Nakos, A Papafitsorou

Higher Geodesy Laboratory, National Technical University of Athens, 157 73 Zographou, Heroon Polytechniou 9, Greece

[Manuscript received February 5, 1987]

The results of studies of the gravity field in the Greek area are presented and discussed in relation to the tectonic background. The occurrence of the African tectonic plate and its subduction under the Aegean together with the Hellenic trench and the Alpine fold, disturb the gravity field of the region at a wide range of wavelengths. The abrupt Moho depth changes indicate among other features a possible lack of isostasy and the need of mass modeling in order to explain the long wavelength variations of the gravity field.

The referenced F.A. anomalies to GRM3L1 geopotential model, truncated at degree 30 were further smoothed by a statistically estimated complete Bouguer reduction with the use of 5'×5' mean topographic heights. The resulted gravity anomaly signal contains major lithospheric information indicated by the directivity diagrams. Statistical evaluation of the distance dependent Bouguer coefficient at 1°×1° blocks indicated the presence of densities in the area between the Hellenic arc and the Alpine fold which can be considerably different from the one used in the standard earth models.

Further research is needed with denser and more extended data.

Keywords: gravity field; Greece; lithospheric signal; modelling

INTRODUCTION

The Greek area, a part of the Eastern Mediterranean, is one of the more interesting areas in Europe from a geophysical point of view. This area has been the object of several geophysical studies (e.g. Papazachos and Comninakis 1971, Woodside 1976, Makris 1973, 1977) which indicate the presence of active tectonic stress fields, unbalanced masses and energy released from tectonic activity at various depths.

The estimation of the earth's gravity field is the main object of physical geodesy and methods that deal with this problem involve the gravity field modeling under the assumption that the anomalous gravitational potential T fulfills Laplace's equation $\nabla T = 0$, at least outside the surface of the earth. These methods are approximation methods for harmonic functions, and no assumption is made about the density distribution which actually generates the gravity field.

For geodesy, the gravity field modeling is a direct problem with unique solution, while for geophysics it is an inverse problem without unique solution. In geophysically complex areas the geodetic gravity field modeling needs a second order approximation, involving the geophysical inversion which is not restricted to the short wavelength variations due to terrain, but it may be needed also for longer wavelengths. These wavelengths can be related to the tectonic features of the region and may come from deep mass sources.

The gravity field of the Greek area, although mostly complicated, is not yet adequately modeled for a geodetic purpose (i.e. representation of an accurate geoid). This is partly due to the great complexity of the area and partly to the fact that the available data belong to different institutions with various objectives. Therefore, a systematic study of an hybrid gravity field modeling/geophysical inversion demands a collaboration of all institutions, in the frame of a long term project.

This work is an attempt to:

- describe the data which are available at the Higher Geodesy Laboratory of the N.T.U. of Athens
- present previous results which were obtained using a part of these data
- present new results in order to extend previous investigations.

The theoretical background consists of statistical concepts at a great part and of geophysical information. Frequent use of related references will prevent repetitions.

It is worth mentioning that in spite of the generally accepted use of the high degree and order geopotential models (G.M.) to refer the gravity field data in modeling problems (e.g. Tscherning 1983, Forsberg 1984, Schwarz 1985), this consideration is not valid for the Greek area. As it will be shown in the following, it seems that local mass modeling would be more appropriate, at least in some regions, in order to replace the medium wavelength variations of the gravity field.

THEORETICAL CONSIDERATIONS

Gravity field modeling is needed in physical geodesy and geophysics. The approach of modeling is different for each purpose. In physical geodesy it is a direct problem in which the disturbing gravitational potential T must be a harmonic function. In geophysics it is an inverse problem, where the observed gravity field must be generated from an assumed mass model.

The gravitational disturbing potential T at a point $P(r,\varphi,\lambda)$ is generated by a density anomaly distribution Δp:

$$\tilde{T}(P) = k \int_V \frac{\Delta p}{r} \, dV \tag{1}$$

where r is the distance between P and the center of mass of the disturbing mass element, dV is the volume of this element, k is the gravitational constant and Δp is the difference between the actual density distribution and a "normal" density distribution which generates the normal potential U

$$\Delta p = p - p_0 \, . \tag{2}$$

Any density distribution Δp can satisfy (1) because any radial symmetric normal density distribution p_0 can generate the normal potential U, provided that the value kM is correct (M is the mass of the Earth). So, p_0 must be chosen.

The potential T can also be expressed by the usual spherical harmonic expansion:

$$\tilde{T}(P) = kM \sum_{n=2}^{nmax} \sum_{m=0}^{n} \left(\frac{R}{r}\right)^n (\bar{C}^*_{nm} \cos m\lambda - \bar{S}^*_{nm} \sin m\lambda) \, P_{nm}(\sin\varphi) \, \cdot \tag{3}$$

The approximation $\tilde{T}(P)$ in (3) is split up as successive approximations with increasing degree in of expansion:

$$\tilde{T}(P) = \tilde{T}_1 + \tilde{T}_2 + \tilde{T}_3 + \ldots \tag{4}$$

where $\tilde{T}_1$, $\tilde{T}_2$ ... are the components relative to the increasing degree n and are related to the depths of the sources of the disturbing mass in the interior of the earth.

The observable gravity field quantities g, N, ξ , n, etc. in the usual spherical approximation are expressed as linear functionals L(T) of T and have different "sensitivity" to the disturbing mass sources. This is because the depth of the source affects differently each of the above quantities (e.g. Meissl 1971), since the physical characters of these quantities are different.

Any set of observed gravity field quantities on the earth can be considered to satisfy a statistical collocation model:

$$x = A\ X + s + n \tag{5}$$

where x = L(T), A X is the trend part, s is the random signal and n is the noise.

Linearization of (5) can be applied when the trend part is properly expressed:

$$x - A\ X = s + n \tag{6}$$

However the trend elimination may be viewed as a structural one in which the components of the parameter vector X

$$X = X\ (x_1,\ x_2,\ x_3,\ \ldots) \tag{7}$$

are related to geophysical characteristics.

So, the traditional reference of L(T) to a geopotential model (G.M.)

$$L(T) - L(T_{GM}) = L(\Delta T) \tag{8}$$

can be viewed as a kind of structural trend elimination for the low-end part of the medium wavelengths of the gravity field (see Table 3.1 in Schwarz 1985). For this aspect, the coefficients C_{nm}, S_{nm} of the spherical harmonic expansion are considered to be related to the depth of the disturbing mass sources which generate the gravity field.

This consideration is opposed to the usual reference of L(T) to high degree G.M. ($n = 180$), not only because of the errors in the estimation of high degree coefficients (e.g. Rapp 1981) but also because the relation between the depth of sources and the affected degree and order of coefficients C_{nm} and S_{nm} is not well defined. One may adopt that for degrees $n \geq 30$ the coefficients contain lithospheric information (e.g. Bjerhammar 1981).

The most important and best known density anomalies are in the earth's interior those associated with topography. They include the gravitational effect of the visible topographic masses (orthometric heights), the bathymetry and the isostatic compensation. These effects account for the major part of the gravity field variation, at least for wavelengths $\lambda < 1000$ km. In a global statistical study for the earth's gravity field (Jordan 1978) it is estimated that about 97 % of the gravity anomalies are due to the lithosphere. However, the gravity anomalies for $\lambda = 500$ to 170 km may result from density variations beneath the lithosphere (Parsons and Daly 1983), while this range shares causes of isostasy and lithospheric flexure for topography (Jordan 1978).

In geophysically complex areas usual characteristics are the thickening of the crust and phenomena in the earth's lower lithosphere which tend to establish the isostatic equilibrium. The isostatic equilibrium is considered as a static, thermal and kinematic one. Both characteristics have as surface expressions the generation of topography and the motion of tectonic units (isostatic motions, rotation of plates). Typical examples of deeply compensated regions (through anomalous density values in upper mantle) are sea trenches.

For such areas the task to model analytically the gravity field may be difficult because:

- medium wavelengths can be associated to different tectonic units which may have been brought to different elevations by vertical actions and compressive forces with source origin at the lower lithosphere
- the wavelengths associated with the topography will be contaminated by crustal flexure and density contrasts which do not belong to the visible masses.

Therefore the linearization of the gravity field modeling involves a wide range of wavelengths-and this problem may be viewed in relation with the statistical information contained in the gravity field functionals L(T). This information is useful for the detection of structural trends and is related to:

- the type of the functional (gravity anomaly, undulation, deflection of the vertical) and its sensitivity to the gravitational attraction of the topographic masses
- the resolution of the data (minimum detectable wavelength)
- the geographical covering of the data (maximum detectable wavelength).

The results of the inversion for medium wavelengths can be interpreted as statistical averages on which the high frequency part of the gravity field is superimposed. The geoid may offer a possibility to check linearity for medium wavelengths through the relation to the undulation of the Moho (e.g. Doufexopoulou 1984).

The covariance functions of the gravity field functionals are widely used for the prediction/estimation of the gravity field. The two basic parameters, the variance C_0 and the correlation distance ξ (e.g. Moritz 1976) control the quality of the above quantities.

The power spectrum of a quantity can be viewed as the decomposition of the variance in narrow bands of frequency. Therefore the variance of an experimental covariance function is a direct measure of the power existing in the data field, for recognizing purposes. The correlation distance indicates the frequencies in which the power is concentrated. A small correlation distance indicates power in high frequencies. So the experimental (empirical) computation of the covariance function (C.F.) can be used as an alternative to the frequency analysis methods (Fourier transforms etc.), especially for recognition. Moreover the computation of the 2-D C.F. allows, in some cases, the detections of structures related to the tectonic background (e.g. Meskó 1977).

In principle, the free air gravity anomalies give anisotropic C.F. and the orientation of anisotropy is related to the topography, provided that no serious geological changes occur in the area under examination. For small areas, the F.A. anomalies are related to the topographic elevations:

$$g_{FA} = a + bh + s \tag{9}$$

where a and b are coefficients and h is the topographic elevation. The coefficient a can be interpreted as a mean Bouguer anomaly for the region, while b is a representative Bouguer coefficient. For the standard density of the surface masses 2.67 gr/cm^3, b is 0.1119 mgal/m. However, when the Bouguer coefficient cannot be assumed as constant, but is varying with the distance, it can be estimated as (Heiskanen and Moritz 1967):

$$b = \frac{Cov(\Delta g, h)}{Cov(h,h)} \tag{10}$$

An interpretation of this relation can be found with the use of the convolution integral of gravity anomaly-topography (e.g. Doufexopoulou 1985). For small areas where the flat earth approximation can be used, the Bouguer coefficient is:

$$b = 2\pi kph \tag{11}$$

where p is the density of the topographic masses.

Thus, when the Bouguer coefficient is estimated analytically for a region with the regression (9), an estimation about the surface mass density can be obtained under the essential assumption of the linear relation between gravity anomaly and topography. If the estimated values of b (or p) differ considerably from the standard ones ($b = 0.1119$ mgal/m, $p = 2.67$ gr/cm^3), either the data are noisy, or the density is not the standardly adopted. However, even in the case of noisy data, the variation of b (or p) at various sample regions in an area indicates the variation of subsurface mass densities.

The covariance function of terrain elevations indicates the terrain variability:

$$c^h(s) = M\left\{ h(\tau) \cdot h(\tau+s)\right\} \quad \text{for } \tau = 0 \text{ to } \tau \max \tag{12}$$

(where $C^h(s)$ is the covariance estimate for distance s, τ is the sampling interval) and can be used for the estimation of the order of terrain corrections in an area (Sünkel 1981) from the formula:

$$\text{T.C.} = 3\pi k p \frac{C_0^h}{\xi} \tag{13}$$

where C_0^h is the variance of the topographic elevations, ξ is the correlation distance, p is the density, and T.C. is the order of the terrain correction.

The order of terrain corrections over different sample regions within an area can be used as a numerical filter to the gravity anomaly data for the elimination of high frequencies.

On the other hand, the selected degree of truncation of the G.M. to refer the local gravity data corresponds to a high pass filtering. Thus, with this kind of crude high and low pass numerical filtering, the gravity anomaly data include the part which is considered as a signal of the local gravity field, and can be related to structural anomalies within the lithosphere.

The computation of 2-D C.F. of the "filtered" gravity data will give azimuth dependent covariance values. These values can be used for the construction of the directivity diagrams (Meskó and Kis 1977) as following:

Diagrams are obtained by summation of covariance values along azimuths:

$$I_R(a) = \int_0^R \varphi(r \cos a, r \sin a)\, dr \tag{14}$$

where (a) is the continuous covariance with arguments (x,y) expressed in polar coordinates. Instead of the continuous function, the experimental values of the covariance are available at distances s = id and orientations a. Therefore:

$$I_R(a) = \sum_{i=0}^{n} \varphi(id,a) \tag{15}$$

where φ (id,a) is the experimental value of the covariance of data points for distance id and azimuth a,d is the data interval. For reasons of statistical stability, the upper limit of summation n should be at least

$$n = \frac{L}{5d} \tag{16}$$

where L is the length of the data block.

The upper limit of summation n acts as a parameter for the identification of linear features. The large peaks in I_R values correspond to linear structural features, provided that n is sufficiently large.

This geophysically originated method can be used to confirm structures (tectonic plate boundaries, faults, etc.) for which results from other methods contradict.

DESCRIPTION OF DATA

For several regions of Greece data files including mean height values are available at the Higher Geodesy Laboratory of the N.T.U. of Athens, These values have been calculated after manual digitization of contour lines from topographical maps. The scale of these maps was selected in respect to the grid size of each file.

The whole procedure includes two phases. The first one concerns the digitization and a linear registration model. In the second phase, the mean height values with their standard deviations are calculated through an algorithm based on the linear integration of contour lines.

The available data files containing mean heights are:

1. 5'×5' grid of mean height values. It is located in Western Greece between $\lambda = 19^0$ to 24^0 and $\varphi = 36^0$ to 42^0. As initial source map, the series of 1:1 M scale bathymetric maps of Mediterranean (I.O.C. (Head Department of Navigation and Oceanography, USSR, 1981)) with 200 m contour line interval was used.
2. 1'×1' grid of mean height values. It is located at Etoloakarnania area and covers a region of 1^0 0.5^0.
3. 15"×15" grid of mean height values. It is located at Zakynthos island and Delvinaki area which extend from $\lambda = 20^0 37'$ to $20^0 57'$ and $\varphi = 37^0 40'$ to $37^0 57'$ and from $\lambda = 20^0 15'$ to $20^0 35'$ and $\varphi = 39^0 45'$ to $40^0 05'$, respectively.

For both 2 and 3 sections the series of 1:50 K scale topographic maps of HAGS with 20 m contour line interval were used as source maps.

The data files containing free air gravity anomalies extend from $\lambda = 20^0$ to 27^0 and $\varphi = 35^0$ to 41^0, and contain 5300 5'×5' mean values, as well as 672 15'×15' means. These files have been created through manual digitization of the free air gravity anomaly map of Greece which is published by the Greek Military Service. The scale of the map is 1:1 M with a contour interval 10 mgal. The uncertainty of the 5'×5' mean values is estimated to 4 mgals (Doufexopoulou 1985). The 15'×15' mean values file is produced from the 5'×5' one by simply averaging the 9 5'×5' values which occur within each 15'×15' block. The uncertainty of the 15'×15' values is 12/9 mgals, applying the law of propagation of variances.

PREVIOUS AND RECENT ANALYSIS AND RESULTS

In the frame of a local gravity field study for the geoid approximation (Doufexopoulou 1985) it was early indicated that the free air anomalies pattern shows anisotropic characteristics in the empirically computed 2-D covariance functions (Doufexopoulou 1982). In addition, strong inhomogeneities were indicated by a wide range of variance value parameters which could not be explained by the terrain. The values of variance generally showd an increase towards East and South and this investigation suggested the need of a more systematic study of the area from a geodynamical aspect.

Although during these computations a digital terrain model for the reduction of the gravity data was not available, the preferred orientation of anisotropies and the inhomogeneity indicated that the reasons for the interpretation had to be looked for also within deeper mass structures than the terrain. The two major tectonic blocks (African and Aegean plates) and the subducting slab of the African plate introduce disturbances of medium wavelengths in the gravity field and the lithospheric signal is masked. So, elimination of structural trends is of importance in order to study in detail the fine structure of the gravity field.

With the use of the Moho depth model and of altimetric undulations, the linear correlation between these data was checked over the African and Aegean plates (Doufexopoulou 1984). This correlation is expected to hold for the flexure model of isostatic compensation (e.g. Sandwell 1984). Results are presented in Table I. No correlation exists over the Aegean while over the Southwestern part of the country the linear correlation is confirmed.

Table I. Correlation between geoid undulations and Moho depths over the African tectonic plate (from Doufexopoulou 1984)

Geoid undulation	Degree of harm. expansion	Correlation coef.
GEM10B	36	0.755
GEM10C	180	0.567
Altimetric (Geos 3+Seasat)	360	0.801
Gravimetric (Stokes)	360	0.711
Gravimetric (collocation)	360	0.814

The geoid can be used for the medium wavelengths study of the gravity field because the undulations N have sources at deep lithospheric features (e.g. Kaula 1972, see also Schwarz 1985

Table 3.1). In addition, the undulations may be considered as low pass filtered gravity anomalies, through e.g. Stokes kernel. The low frequency part of the geoid (degrees ≤ 36) can be well modeled with the use of G.M. because the C_{nm} , S_{nm} coefficients are well defined in those G.M. which also contain altimetric data. In addition, the spherical harmonic coefficients $n < 36$ come mainly from lower lithosphere and deep mass layers.

The technique which is mostly followed in local gravity field modeling concerns the combination of a G.M. and local data. The G.M. is used as a reference field for the local data. The remaining residual gravity field data can be considered as a signal presenting the local features of the field. High degree and order ($n \geq 180$) G.M. may not be suitable for this purpose, in spite of the advantages it may offer (e.g. decrease of local data coverage, use of flat approximation, etc.). These advantages may be questioned from the aspect of geophysical inversibility of high degree coefficients, as well as the increase of errors in the coefficients above $n = 120$ (Rapp 1981).

For the Greek area the choice of a conforming reference G.M. was studied from the aspect of its geophysical "inversibility" and the power distribution at different degrees of expansion. Four G.M.-s were studied, GEM10B, GRIM3B, GRM3L1 (n=36) and RAPP81 (n=180) (Doufexopoulou and Papafitsorou 1986). As criteria for the choice were used:

- the correlation of undulation components between different degrees of expansion of the G.M with the Moho depths
- the behaviour of the index of inhomogeneity for various reference degrees of the local 15'×15' anomaly data. As index of inhomogeneity the ratio of the higher to the lower variance of referenced anomalies was considered. The higher and lower variances refer to three subregions, into which the whole area was divided, in order to investigate the inhomogeneity of the gravity field
- the construction of the variance spectra of the geoid undulations for the G.M.

The details of these computations can be found in the above mentioned reference. Significant correlations obtained are presented in Table II. In Table III the variances referred to G.M. local anomalies are shown for the four models and three subregions. Figure 1 shows the index of inhomogeneity for the RAPP81 G.M.

Table II. Correlation coefficient between computed components of undulation from G.M. and Moho depths for African and Aegean tectonic plates

Region \ GM	expan.	GRM3L1	GRIM3B	GEM10B	RAPP81
	22-30	0.174	0.201	-	0.300
African	30-36	0.876*	0.819*	0.794*	0.623*
	45-60				0.697*
	22-30	0.648*	0.648*	-	0.604*
Aegean	30-36	0.552	0.529	0.808*	0.842*
	45-60				0.179

*represents significant (numerical) correlation

Table III. Variances of Δg(F.A) referenced to GM for regions I, II, III (Local field of 15'×15' anomalies. Unit: mgal^2)

Region \ Model	n	GRM3L1	GRIM3B	GEM10B	RAPP81
I	30	821	838	-	806
	36	669	704	871	678
II	30	7574	7818	-	7043
	36	7132	6999	7590	6840
III	30	882	959	-	800
	36	5835	530	941	591

Since the Greek area was recently partly covered with 5'×5' mean topographic heights (or depths), a further analysis of the gravity field has been done. The studied area extends from $\varphi = 38^{o}$ to 41^{o} and from $\lambda = 20^{o}$ to 23^{o} and includes

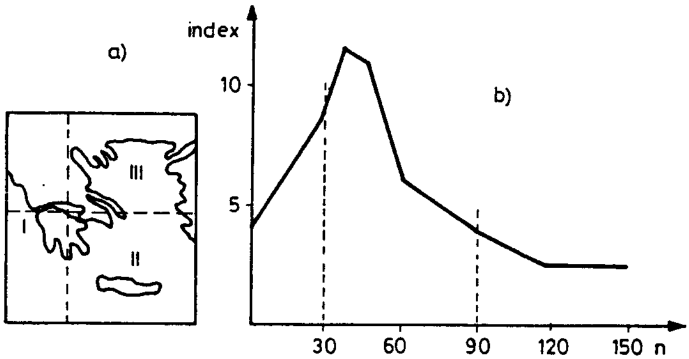

Fig. 1. a) Division of Greece in regions I, II, III for studying the inhomogeneity of gravity anomaly field. b) Index of inhomogeneity, for the Rapp81 G.M., of the local gravity anomaly field. (Higher/lower variance value of referenced gravity anomalies for regions I, II, III)

part of the Alpine fold, as well as major tectonic faults and plate boundaries (Fig. 2). For this area both 5'×5' mean free air anomalies and topography exist. The Moho depths, estimated from seismic and gravity data (Makris 1973) are presented in Fig. 3.

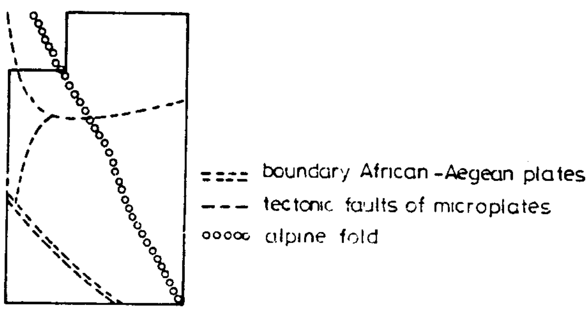

Fig. 2. Main pattern of the region in the present study

The main purpose of this study was to create a file of gravity anomalies whose major variations could be attributed to the lithosphere for further modeling. For that, GRM3L1 G.M., truncated at $n = 30$, was at first subtracted from the mean

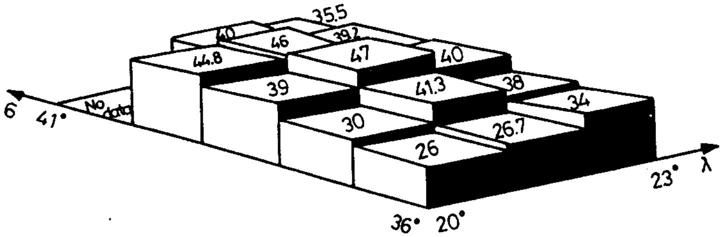

Fig. 3. Moho depth values (km)., Makris (1973)

5'×5' free air anomaly values and the referenced 5'×5' Δg^r's:

$$\Delta g^r = \Delta g - \Delta g_{GRM3L1}$$

are considered to contain information coming mainly from the lithosphere and the topography (Figs 4, 5). The topography was used to estimate a crude complete "Bouguer" reduction (plate and terrain correction) (Fig. 6). The subtraction of these reductions from the Δg^r's (Fig. 7) acts as a low pass filter to the referenced gravity anomalies, and so the major part of the terrain influence is reduced. The process is as follows:

In each $1^o \times 1^o$ block of the study area the mean $1^o \times 1^o$ height was subtracted from the original 5'× 5' mean height values of the block. The $1^o \times 1^o$ local mean topography was preferred to the global $1^o \times 1^o$ values of the spherical harmonic expansion because it represents better the local topography in this complex area.

A covariance and cross covariance computation for (Δg,h) and (h,h) was performed for each $1^o \times 1^o$ block and the correlation distance ξ and variance C_0^h were found. Thus, the order of the terrain correction for each $1^o \times 1^o$ block was computed from Eq. (13). In this computation the standard rock density 2.67 gr/cm^3 was used. For two of the blocks the order of terrain correction (for the standard density) is larger than the uncertainty of the data (7 and 12 mgals). The isolines of the so computed filtered Bouguer map fit well to the analytically computed Bouguer anomalies of a detailed gravity survey for Peloponesos (Makris et al. 1973).

The relation (10) was used for an empirical estimation of the Bouguer coefficient in each block. Naturally, the wavelengts

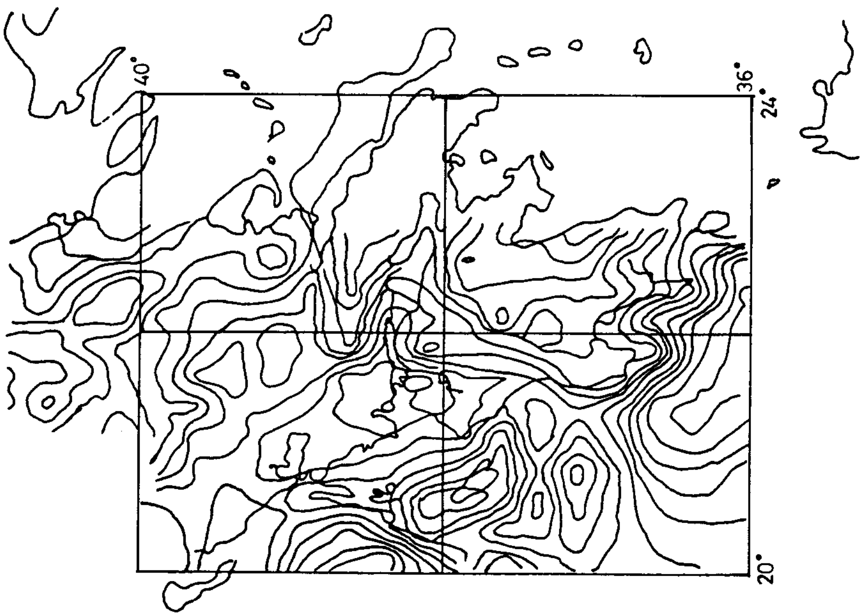

Fig. 4. Free Air Anomalies (Contour interval 20 mgal)

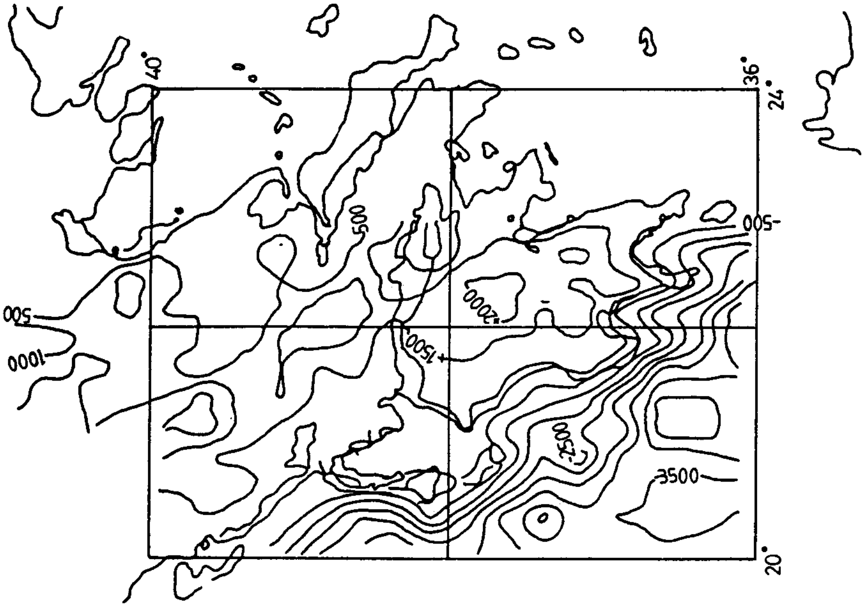

Fig. 5. Topography (Contour interval 500 m)

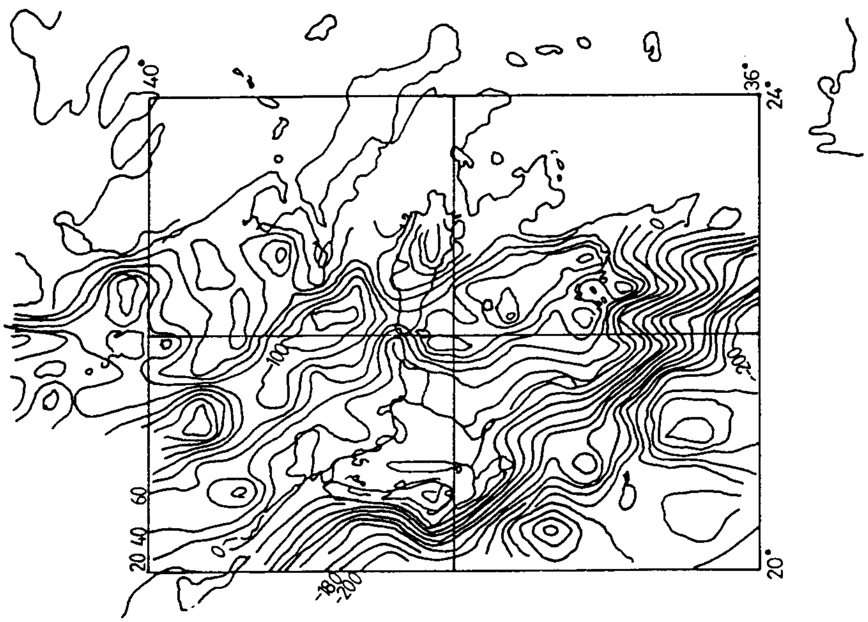

Fig. 6. Terrain Reductions (Bouguer plate + Terrain Corr.) (Contour interval 20 mgal)

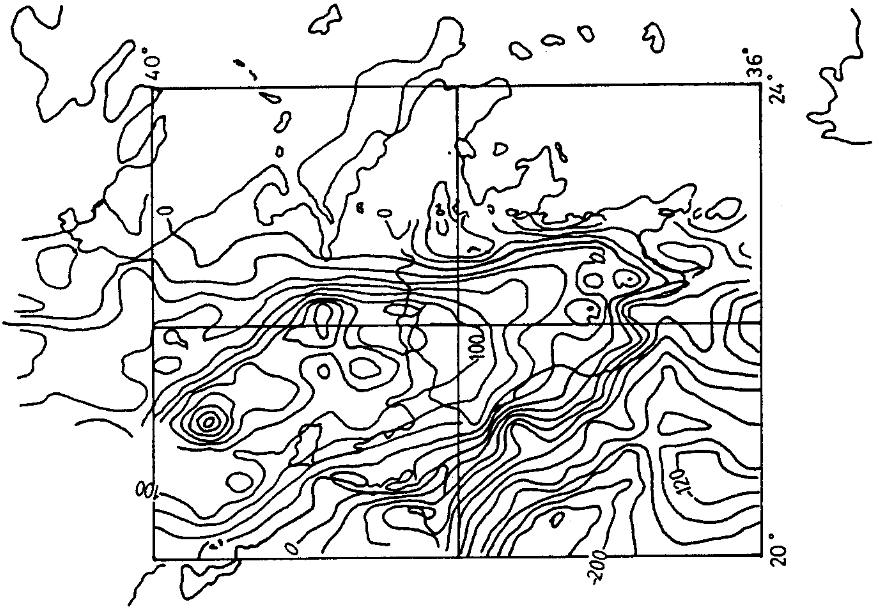

Fig. 7. Residual Gravity Anomalies (Contour interval 20 mgal)

existing in the data to not allow an absolute estimation of the coefficient, but it was expected that some information about the density disturbances could be received from the variations of the so-computed b values in each block. The results of this computation are presented in Fig. 8. Abrupt variations of coefficient b occur in two blocks, while in one block there exists a discontinuity from positive to negative values. The three blocks are located at the South-western part of the area, between the boundary of the African and the Aegean plates and the Alpine fold (Fig. 8).

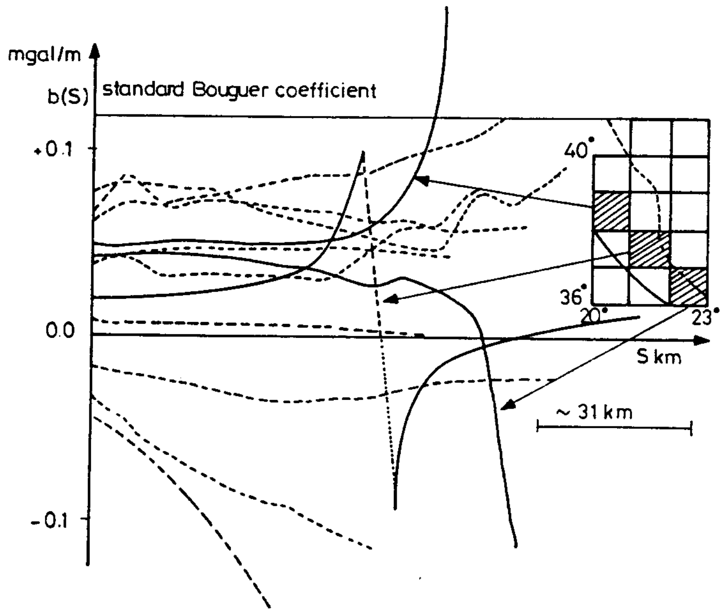

Fig. 8. Plots of distance dependent Bouguer coefficients, statistically derived, for all the $1^{\circ}\times1^{\circ}$ blocks. Shaded blocks indicate possible presence of disturbing masses, corresponding to full-line Bouguer coefficient function in the Fig. 8

After the application of the high and low pass "filters" on the data, the anomalies are considered to be mainly lithospheric signals. In order to check this consideration, the empirical 2-dimensional covariance function of the "filtered" data was computed for three regions within the area, and directivity diagrams were plotted, according to Eq. (15). The azimuths along which the covariance values were calculated are at every 22.5°.

In the northern region (2°× 2°) the preferred azimuth is North-South. For the southern region (3°× 3°) the preferred azimuth is at 135°, almost parallel to the boundary of the African and Aegean tectonic plates. However, for the middle region (3°× 3°) the preferred azimuth of the 2-D covariance function is slightly pronounced at 157.5°, while the directivity diagram has an elliptical shape with small eccentricity. Since within this region the tectonic pattern is more complicated (see Fig. 2) a recomputation of the directivity diagram was done for every 10°, in order to distinguish other important orientations which could be related to the tectonic features. The directivity diagrams are presented in Fig. 9.

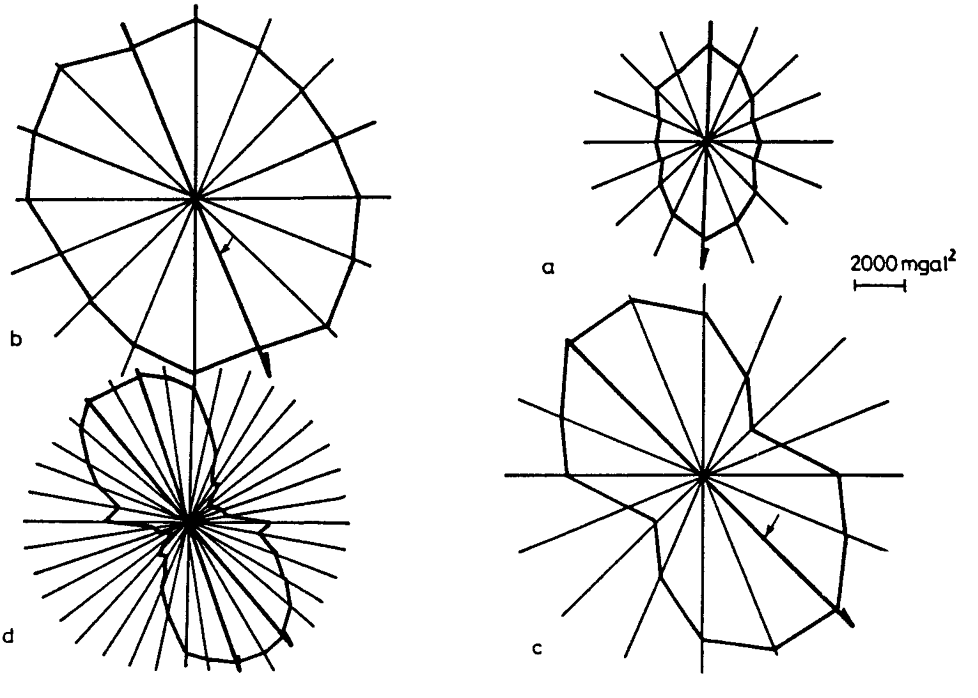

Fig. 9. Directivity for a (north), b (middle), c (south) region, d (as c with higher resolution in directivity azimuth). Arrows present significant directions related to linear features

CONCLUSIONS AND DISCUSSION

It should be pointed out that the rather large grid (5'×5') of the mean values in gravity anomaly and topography does not allow the study of the very short wavelength variations of the gravity field. Since these variations are due to the terrain, the statistically reduced gravity anomalies can be considered as a partly filtered lithospheric signal.

In spite of this problem with the original data files, the tectonic background of the Greek area gives strong enough signal and it is possible to get significant indications on the order of wavelengths which disturb the regional gravity field.

From Table II it can be observed that longer wavelengths disturb the gravity field in the Eastern part of the country, but the total power of the gravity field, as indicated by the variance values of gravity anomalies (Tables III and IV) is considerably lower than that in the Western part (region II in Fig. 1). This suggests that the variations in the Western part are due to shallower masses than the ones in the Eastern part.

Table IV. Variances of Δg(F.A.) referenced to RAPP81 for various degrees of truncation and for regions I, II, III (unit: $mgal^2$)

RAPP81	30	36	45	60	90	120	150	Local data
I	806	678	718	768	621	492•	621	1557
II	7045	6840	5632	4339	2384	1437•	2384	6904
III	800	591	499•	726	655	548	586	1545

The variations of the inhomogeneity index (Fig. 1) indicate that high inhomogeneity is introduced within the whole area when the local gravity anomaly data are referred to a G.M. of degrees 30 ÷ 90 of the harmonic expansion. The corresponding wavelengths are 1200 ÷ 400 km (following the empirical rule $\frac{180}{n}$). For degrees greater than 90 of the reference G.M., the residual field becomes smooth (Table IV) but whithout any significance for inversion. However, the variance of the referenced gravity anomalies in region II is still high, suggesting that there may exist local sources. An optimal degree of the reference G.M is 30 ÷ 36 degrees, if the power sources of the gravity field are to be studied. From the four checked G.M-s, the GRM3L1 seems to fit better in the Greek area.

The statistically estimated order of terrain corrections (Table V) is greater than the uncertainty of the data in the South-western part of the region(recent study) within the same blocks for which the statistical estimations of the distance varying Bouguer coefficient show abrupt or discontinuous changes. These blocks (Fig. 10) are located between the two main plates' boundary and the Alpine fold. A mass model should be needed to interpret the gravity field there.

Since the critical wavelengths of the gravity field variations are 1200 ÷ 400 km, the "filtered" (referenced to GRM3L1 and Bouguer reduced) gravity anomalies should contain lithospheric signal. This is indicated by the directivity diagrams (Fig. 9). The ones for the middle and southern region give significant azimuths which are almost parallel to the boundary

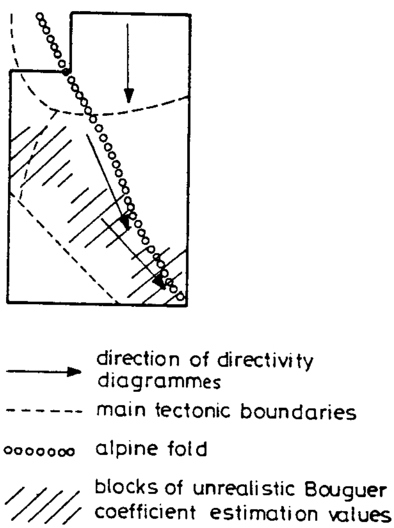

Fig. 10. Direction of directivity diagrams and the pattern of main tectonics on the region in study

Table V. Statistical parameters for topography, $1^{o}\times1^{o}$ blocks, $5'\times5'$ samples and variances of "filtered" gravity anomalies (present work)

Area, top left corner lat, long	Mean elevation $1^{o}\times1^{o}$ (m)	Variance m^2	Correlation distance (arcmin)	Order of terrain correction (mgal)	Type of region	Variance "filtered" gravity anomalies	Ratio: Corr. distance sampling interval
41^{o}, 21^{o}	830	87.796	9.69	2	land	5475 $mgal^2$	1.938
41^{o}, 22^{o}	688	182.857	13.69	2	land	* 711 $mgal^2$	2.738
40^{o}, 20^{o}	988	253.525	13.46	3	land	9233 $mgal^2$	2.692
40^{o}, 21^{o}	970	201.344	15.96	2	land	15622 $mgal^2$	3.192
40^{o}, 22^{o}	318	77.185*	6.00	2	land	* 1150 $mgal^2$	1.200
39^{o}, 20^{o}	334	1247.767	28.48	7	sea	2586 $mgal^2$	5.696
39^{o}, 21^{o}	819	175.385	19.35	2	land	12836 $mgal^2$	3.870
39^{o}, 22^{o}	387	372.585	9.97	6	land	* 3887 $mgal^2$	1.994
38^{o}, 20^{o}	-860	1508.676	24.24	10	sea	28512 $mgal^2$	4.848
38^{o}, 21^{o}	381	634.094	28.88	4	sea	4435 $mgal^2$	5.776
38^{o}, 22^{o}	429	225.715	15.57	2	land	* 3365 $mgal^2$	3.114
37^{o}, 20^{o}	-2212	65.786*	12.72	1	sea	23277 $mgal^2$	2.550
37^{o}, 21^{o}	-194	1819.098	25.56	12	sea	14936 $mgal^2$	5.112
37^{o}, 22^{o}	697	1572.357	21.16	12	sea	* 3567 $mgal^2$	4.232

of the tectonic plates. The diagram for the northern region gives a N-S azimuth, for which there is no clear explanation, or the origin lies within the thick crust.

The gravity field of the Greek area is suggested to be object of further research, priority given to the computation of isostatic gravity anomalies, as soon as the computation of mean heights is completed. Standard isostatic models (Pratt or Airy) are not expected to give a smooth gravity anomaly field. Seismic information together with a mass model (considering e.g. the lithospheric flexure) may give satisfying results in the gravity field interpretation. The identification of the isostatic or tectonic origin of mass disturbances may assist the geodynamical interpretation of time dependent control networks. Collaboration with scientists from other geo-sciences is important for the investigation of the gravity field.

REFERENCES

Bjerhammar A 1981: Longwave heterogeneities as seen in the upper mantle. 7th E.G.S. Meeting, Uppsala, Sweden

Doufexopoulou M 1982: In: Proceedings of the III Inter. Symposium "The use of artificial satellites for Geodesy and Geodynamics", Hermioni, Greece

Doufexopoulou M 1984: In: Proc. of the Intern. Symposium "Space techniques for geodynamics", Tome 1, Sopron, Hungary

Doufexopoulou M 1985: Study of the gravity field in Greece for the geoid approximation (in Greek). Ph.D. Thesis, N.T.U. of Athens

Doufexopoulou M, Papafitsorou A 1986: Inversibility of geopotential models for local gravity field approximation. Presented at the Intern. Symposium "The figure and dynamics of the Earth, Moon and other planets", Prague, Czechoslovakia

Forsberg R 1984: Local covariance functions and density distributions. Department of Geodetic Sciences, O.S.U. Scientific report No. 6, 1984, Columbus, Ohio

Heiskanen W, Moritz H 1967: Physical Geodesy. W H Freeman and Company, San Francisco

Jordan S K 1978: J.G.R., 83, 1816-1824.

Kaula W 1972: In: The nature of the solid earth. Ed. by E Robertson, U.S. Geological Survey, Silver Spring Maryland

Makris J 1973: Bull. Geol. Soc. of Greece, 10, I. 206-213.

Makris J 1977: The crust and upper mantle of Aegean region obtained from deep seismic soundings. Publ. Inst. Geoph. Pol. Acad. Sci. A-4 (115).

Makris J, Mavridis L, Menzel H, Stavrou A, Veis G 1973: Zeitschrift für Geophysik, 39, 929-936.

Meissl P 1971: A study of covariance functions related to the Earth's gravitational potential. O.S.U. Report, No. 151, Columbus, Ohio

Meskó A, Kis K 1977: Acta Geol. Acad. Sci. Hung., 21, 325-335.

Moritz H 1976: Covariance functions in Least Squares Collocation. O.S.U. Report, No. 242, Columbus, Ohio

Papazachos B C, Comninakis P K 1971: J.G.R., 76, No 35, 8517-8533.

Parson B, Daly S 1983: J.G.R., 88, B2, 1129-1144.

Rapp R 1981: The Earth's gravity to degree and order 180 using Seasat Altimeter data, terrestrial gravity data and other data. Report No. 322, Department of Geodetic Sciences, O. S.U., Columbus, Ohio

Sandwell D 1984: J.G.R., 89, B2, 1089-1104.

Schwarz K P 1985: In: Proceedings of Local gravity field approximation, Beijing China

Sünkel H 1981: Point mass models and the anomalous gravity field. Department of Geodetic Science and Surveying, Report No. 328, O.S.U., Columbus, Ohio

Tscherning C 1983: In: Proceedings of the 18th General Assembly of IAG-IUGG, Hamburg

Woodside J 1976: J.G.R., No. 47, 1947-1968.